Eur. Phys. J. B **36**, 105–113 (2003)
DOI: 10.1140/epjb/e2003-00322-1

THE EUROPEAN PHYSICAL JOURNAL B

Jamming transition of a granular pile below the angle of repose

S. Deboeuf[1], E.M. Bertin[2], E. Lajeunesse[1], and O. Dauchot[2,a]

[1] IPGP, CNRS/INSU UMR 7580, 75005 Paris, France
[2] DSM/SPEC, CEA Saclay, 91191 Gif-sur-Yvette, France

Received 30 May 2003 / Received in final form 9 September 2003
Published online 19 November 2003 –

Abstract. We experimentally study the relaxation towards mechanical equilibrium following the surface avalanche of a granular pile and discuss it in the general context of glassy materials and jamming transition. Two coexisting dynamics are observed in the surface layer: a short time exponential decay related to rapid isolated grains displacements, and intermittent reactivation bursts consisting in spatially correlated moves. The competition of both dynamics results in long-lived intermittent transients, the total duration of which can last more than a thousand of seconds. The typical time-scales, and the two-time relaxation function of these transients are measured. Analyzing the response of the surface layer to localized perturbations provides new evidence for spatial correlations. We further analyse the relaxation function in a probabilistic framework, which allows to discuss different possible scalings according to the choice of specific hypothesis. Following some considerations on the observed time-scales, we finally discuss the similarities with aging systems which are suggested by our description of the observed dynamics.

PACS. 05.20.-y Classical statistical mechanics – 45.70.-n Granular systems – 45.70.Cc Static sandpiles; granular compaction – 64.70.Pf Glass transitions

1 Introduction

Dry, non-cohesive granular materials can flow like a liquid but can also sustain a finite angle of repose θ_r. The large number of degrees of freedom suggests to think in terms of phase transition: for a pile slope $\theta > \theta_r$, surface layers flow downhill, whereas for $\theta < \theta_r$, these layers "freeze" and the pile behaves like a solid. Bak et al. [1] proposed the idea that a granular pile "self-organizes" into a critical state at the angle of repose. However, a number of experimental works [2–6] have concluded that successive avalanches exhibit more complex dynamics – including hysteretic behaviours.

In this paper, we reconsider the avalanching pile problem but, instead of focusing on avalanches statistics, we study the relaxation of the pile towards mechanical equilibrium following one single avalanche. We first show that the dynamics exhibits non-trivial relaxations and is much slower than expected given the "microscopic" time-scale. We observe two coexisting dynamics in the surface layer: a short time exponential decay related to rapid independent grains displacements, and intermittent bursts which temporarily reactivate the pile dynamics. These bursts are identified with correlated movements in space and time. Perturbation experiments allow to confirm the emergence of strong spatial correlations when increasing the pile slope. The two time-scales associated with both dynamics are measured. We then consider the two-time relaxation function, given by the total number of displacements between time steps t_w and $t_w + t$. At first sight, it exhibits the scaling expected for a pure irreversible dynamics, in apparent contradiction with our direct observation of reverse processes. Further analysis reveals that it also scales as predicted by a simple argument consistent with both a globally irreversible dynamics and instantaneous reactivation processes. We finally discuss the possible origins of the observed time-scales, and the analogies of the present granular system with glassy materials. More specifically, the above relaxation function is related to a correlation function similar to that appearing in aging systems.

The experimental setup is described in Section 2 and the observations are reported in Section 3. Section 4 is then devoted to the more detailed analysis. Finally, the results are discussed in Section 5, emphasizing possible connections with glassy dynamics.

2 Experimental setup

The experimental setup shown in Figure 1 consists in a rotating drum of internal diameter $D = 450$ mm and thickness $\delta = 22$ mm, half-filled with steel beads of diameter $d = 3 \pm 0.025$ mm and density $\rho = 7.8\ \mathrm{g\,cm^{-3}}$.

The friction coefficient and the coefficient of restitution of the beads are respectively $\mu = 0.2$ and $e = 0.92$.

[a] e-mail: olivier.dauchot@cea.fr

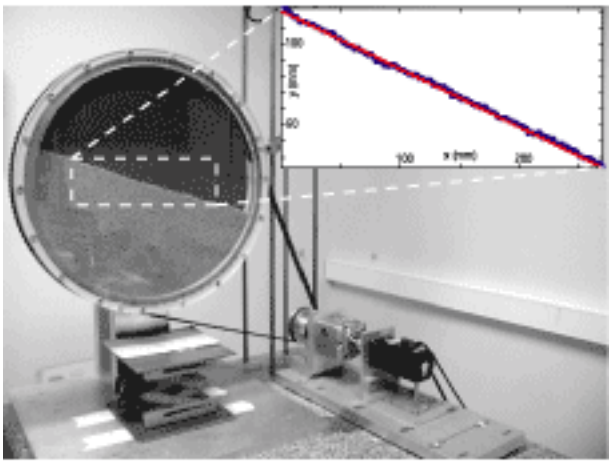

Fig. 1. Picture of the experimental setup. The inset displays a typical acquisition of the pile slope.

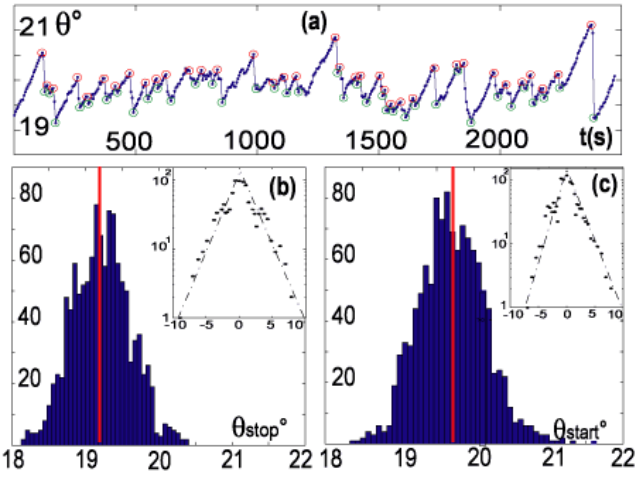

Fig. 2. (a) pile slope angle $\theta(t)$ (°) as a function of time. (b), resp.(c) histograms of θ_{stop}, resp. θ_{start}. Insets are log-lin plots of the reduced centered distributions.

A DC motor drives the drum clockwise or anticlockwise at angular velocities as low as $\Omega = 0.01°/s$. The pile slope is set to any given value smaller than the repose angle by braking the drum. The pile is lightened by a continuous halogen lamp located far enough from the drum to prevent heating. Also the lab temperature is regulated at a constant value 20 °C. The experimental area of interest is filmed either by a standard CCD camera (768×572 pixels at 25 i/s) or by a fast one (480×210 pixels at 1000 i/s) aligned along the axis of the drum. In both cases, the camera focus is set to have a spatial resolution of 0.5 mm per pixel. Image acquisition and processing allow to extract the pile slope, the surface roughness and to detect the pixels where a displacement as small as 25 μm has occurred.

The surface detection takes advantage of the gradient of the light intensity fluctuations which are maximum at the surface of the pile $S(x)$. The averaged slope of the pile θ is then deduced from a linear least square fit of $S(x)$ while the surface roughness r is given by the average deviation around the mean slope. Beads displacements are detected using an images difference method already described in [7]. In principle, measuring the intensity difference between two consecutive images of the pile allows to identify the region where beads displacements have occurred. In practice, the noise caused by lighting inhomogeneities, camera intrinsic vibrations and data-acquisition must be reduced. This is achieved by acquiring two consecutive sequences of n images: $n = 25$ (respectively $n = 200$) for the standard (respectively the fast) camera. The two sequences are averaged resulting in two frames. Substracting them and binarizing them so as to remove any remaining noise leads to the detection of the area where displacements have occurred. n is chosen according to a compromise between the noise/signal ratio and the temporal resolution. The sensitivity of this detection method is calibrated by translating the camera with a micrometric translator: any displacement larger than 20 μm is spotted unambiguously. The method takes advantage of the whole range of the acquisition dynamics to detect displacements much smaller than the pixel size. The counterpart is that only the existence of such small displacement is detected, but not its amplitude.

3 Experimental results

3.1 Repose and avalanche angles

We first measure the repose and avalanche angles θ_r and θ_a of the granular pile. The drum is rotated at a very low velocity ($\Omega = 0.01°/s$), so as to be in the intermittent regime of macroscopic avalanches [6,8,9]. The pile slope $\theta(t)$ and the surface roughness $r(t)$ are extracted every 5 s from two experimental runs of 12 hours each.

A typical sequence of the pile slope evolution $\theta(t)$ is displayed in Figure 2a. In such a low rotation regime, $\theta(t)$ increases linearly with time at the rate Ω until an avalanche occurs at θ_{start} and the slope relaxes towards a stopping angle θ_{stop}. The pile roughness remains in the order of half a grain diameter and no correlations between $r(t)$ and $\theta(t)$ or their temporal derivatives emerge. We filter the events for which the pile slope variation $(\theta_{start} - \theta_{stop}) < 0.1°$, which correspond to a local slope rearrangement implying only a few beads, and we end with a thousand of events identified as avalanches. The resulting histograms of θ_{start} and θ_{stop} – Figure 2b, c – exhibit exponential tails (see insets), which could indicate non-trivial fluctuations in θ_{start} and θ_{stop}. Still, in absence of a better definition, we choose to estimate the repose and avalanche angles θ_r and θ_a as the averaged values of respectively θ_{stop} and θ_{start} leading to $\theta_r = 19.2° \pm 0.2°$ and $\theta_a = 19.7° \pm 0.2°$. The relatively small difference between θ_a and θ_r could be explained by the large restitution coefficient of our steel beads.

3.2 Relaxation dynamics

In order to investigate the relaxation of the pile following an avalanche, the drum is rotated at constant velocity (1°/s) during a few minutes, so that several avalanches

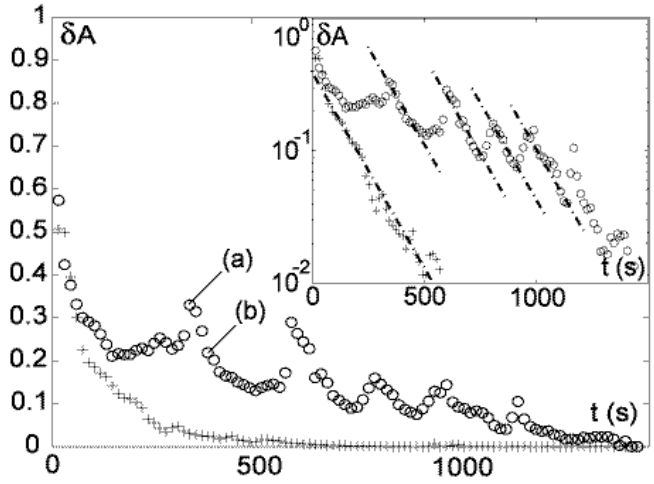

Fig. 3. The mobile volume fraction evolution $\delta A(t)$ for two different realizations at similar pile slopes: ($\circ$) $\theta = 15°$; (+) $\theta = 16.5°$. Inset is the log-lin plot of the same data. Notice the exponential decay rate, which is identical in the monotonous case (+) and in the intermittent case ($\circ$).

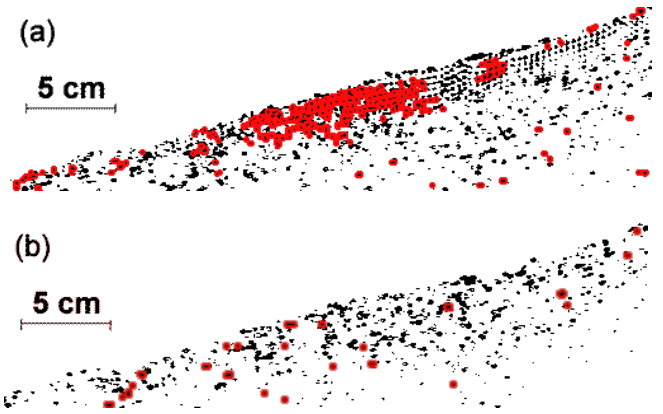

Fig. 4. Displacements in the pile at the time steps labelled (a) and (b) in Figure 3. The dark pixels correspond to positions where a displacement has occurred in the 15 s preceding the given time step. The red (light) overlay indicates the pixels, where displacements have occurred successively during 30 s following the given time step (see text for details).

have occurred. The drum is then stopped just after an avalanche ($\theta = \theta_{stop}$) and rapidly rotated backwards down to the desired angle $\theta < \theta_{stop}$. The relaxation is recorded with the standard CCD camera. Consecutive sequences of $n = 25$ images of the pile are taken every 15 s. Beads displacements occurring between two sequences are detected following the procedure described in Section 2. As a result a set of binary images is obtained where black pixels indicate positions where displacements have occurred.

The "mobile volume fraction" of the pile $\delta A(t)$ (i.e. the fraction of beads that have moved between the two acquisitions) is computed as the total number of dark pixels normalized by the total number of pixels covering the pile. Figure 3 displays two typical records of $\delta A(t)$ as observed for two realizations of the pile relaxation with similar slopes $\theta = 15°$ and $\theta = 16.5°$. Note how the choice of an irregular relaxation realization for $\theta = 15°$ and a regular one for $\theta = 16.5°$ emphasizes the variability observed among realizations, in this slope range. During the very first time steps the relaxation process is identical in both records: the bulk of the pile relaxes rapidly from bottom to top on time-scales in the order of the 15 s delay between two consecutive images acquisitions. It involves isolated beads displacements on time-scale even shorter and of amplitude much smaller than the bead diameter. The relaxation process then slows down in a subsurface layer of thickness $[10 - 20]$ beads diameters. In contrast with the bulk, the subsurface layer may relax very differently from one realization to another as illustrated on the two realizations presented in Figure 3. In the following, we focus on the relaxation in the subsurface layer. In one case, one observes a simple exponential decay of the subsurface layer activity with a characteristic timescale $\tau_\downarrow$ which in the present case is in the order of 200 s. In the other case, the pile activity evolution is more complex: intermittent bursts interrupt periods of exponential decay, with the same time-scale as in first case (see inset of Fig. 3). The competition between the exponential relaxation and the reactivation bursts results in a much slower relaxation lasting up to 30 minutes.

A visual inspection reveals that the reactivation bursts correspond to collective motions of grain clusters whereas the exponential decay observed between two bursts – or when there is no burst at all – involves individual beads displacements. This is illustrated in Figure 4, which displays the binary pictures of two time steps – (a) during a burst event, (b) during an exponential decay period. The mobile volume fraction illustrated by the relative number of dark pixels, δA is in the same order and their spatial distributions are very similar. On these pictures, the red (light) overlay indicates the areas, where the same pixels have successively record displacements during 45 s (15 s before and 30 s after the given time step). In the case of the burst event, and in contrast with the exponential decay case, those displacements last in time and are spatially correlated, in the form of grains clusters.

We now investigate the influence of the pile slope on the relaxation dynamics by performing 185 realizations with $\theta_o \in [0°, \theta_r]$. As shown in Figure 5, the probability of observing intermittent dynamics increases with the pile slope. No intermittent dynamics could be observed for $\theta_o < 5°$ – most likely a statistical effect.

Figure 6a shows the averaged characteristic relaxation time of the exponential decay $\tau_\downarrow$ as a function of the pile slope. It increases significantly from 50 s for $\theta = 0°$ to 250 s when θ approaches the repose angle and can be fitted by a power-law in $(\theta_r - \theta)^{-1}$. By contrast, the reactivation process time-scales do not exhibit significant variations with θ. The distribution of time intervals between two successive bursts, shown in Figure 6b, exhibits an exponential tail, $P(T) \sim e^{-T/\tau_b}$, where $\tau_b = 100$ s is the typical waiting time between two successive bursts.

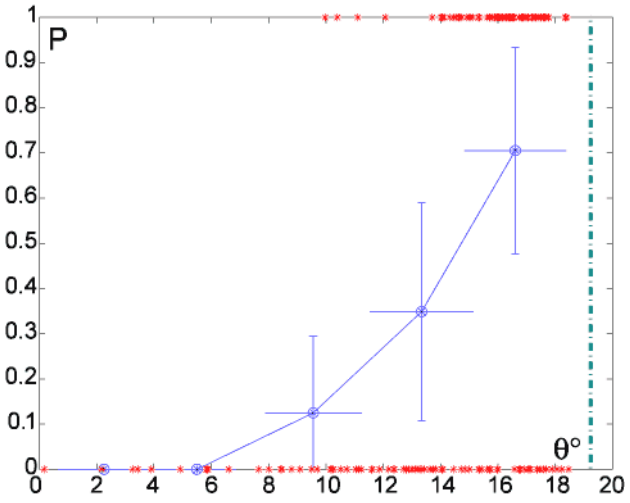

Fig. 5. Probability of observing an intermittent relaxation as a function of the pile slope. The crosses showing each realization are set to 0 for simple exponential decay and to 1 for intermittent dynamics. The vertical dash-dotted line indicates the angle of repose $\theta_r = 19.2°$.

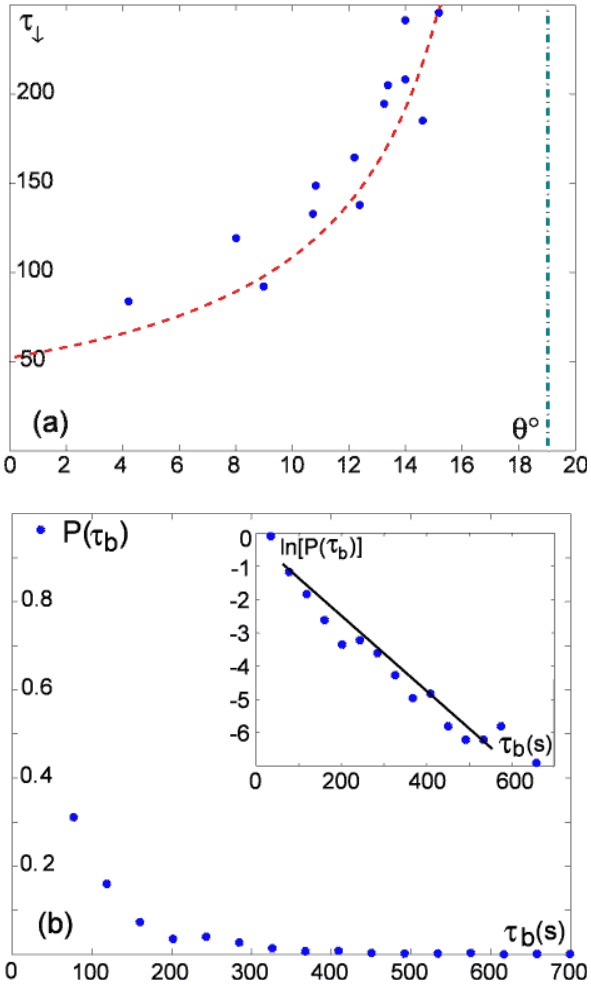

Fig. 6. (a) Averaged relaxation time for exponential decay realizations as a function of the pile slope and (b) probability distribution of the time intervals between bursts in the case of intermittent dynamics.

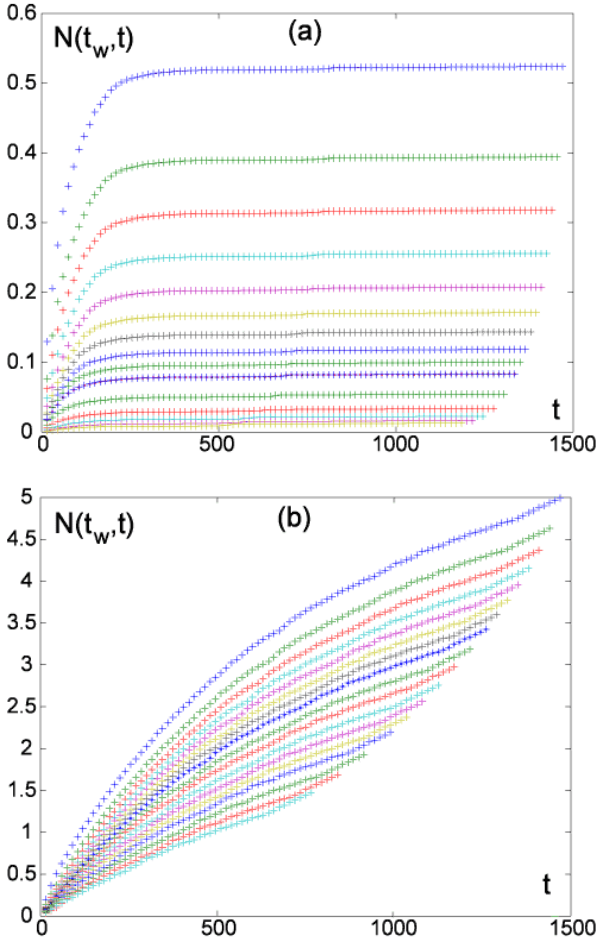

Fig. 7. $N(t_w, t)$, averaged number of displacements per pixel between times t_w and $t_w + t$ plotted vs. t increasing t_w from top to bottom curve: (a) exponential decay case and $\theta < 5°$, $t_w \in [15\text{ s} \rightarrow 180\text{ s}\,(15\text{ s steps}), 180\text{ s} \rightarrow 300\text{ s}\,(30\text{ s steps})]$ (b) intermittent dynamics case and $\theta > 13°$, $t_w \in [15\text{ s} \rightarrow 270\text{ s}\,(30\text{ s steps}), 270\text{ s} \rightarrow 450\text{ s}\,(45\text{ s steps}), 450\text{ s} \rightarrow 750\text{ s}\,(75\text{ s steps})]$.

Interestingly the pile slope for which the monotonous relaxation time $\tau_\downarrow$ becomes in the order of the characteristic time interval between two bursts τ_b coincides with the angle $\theta \approx 10°$ at which the probability of observing bursts during the relaxation becomes significant (> 0.1). This indicates that bursts only occur when the relaxation process is still active, in agreement with direct observations.

The relaxation being a non stationary process, it is a priori better characterized by a two-time relaxation function. Experimentally, it is convenient to measure $N(t_w, t)$ the averaged number of displacements per pixel between times t_w and $t_w + t$, given by:

$$N(t_w, t) = \left\langle \int_{t_w}^{t_w+t} \delta A(u) du \right\rangle \qquad (1)$$

where the brackets denote ensemble average over realizations with characteristic time-scales of the same order. We compute $N(t_w, t)$ for both types of relaxation. For the exponential decay case (Fig. 7a), we average over all realizations obtained for $\theta < 5°$. For the intermittent dynamics

case (Fig. 7b), we average over the intermittent realizations obtained for $\theta > 13°$.

In the first case, $N(t_w, t)$ rapidly saturates whatever the value of t_w and remains smaller than one, which indicates that displacements occur in average less than once at any given position. This is in agreement with the picture of isolated and uncorrelated moves as described above for the exponential decay dynamics. In the second case, the saturation occurs much later. Also $N(t_w, t)$ becomes larger than one, which reflects the possibility of several displacements at a given position. In both cases, $N(t_w, t)$ is reasonably well described by the scaling expected in the case of a purely irreversible process:

$$N(t_w, t) \propto e^{-t_w/\tau}(1 - e^{-t/\tau}). \qquad (2)$$

According to this scaling, the best fit of the data in Figure 7 leads to an estimation of the relaxation characteristic time-scale $\tau = 73$ s for the small pile slopes (Fig. 7a) and $\tau = 725$ s for the large pile slopes (Fig. 7b).

3.3 Response of the pile to a localized perturbation

It was shown above, that the correlated events involved in the non-trivial relaxations concentrate into the surface layer. Here we expect to observe some alternative evidence of these spatial correlations. Therefore, we probe the response of the subsurface layer, to a localized and instantaneous disturbance, during the relaxation. We let a bead fall on the pile surface from a height of 2 cm, with zero initial velocity. The whole procedure is recorded by the 1000 i/s camera during 1 s covering the impact of the incident bead. The image difference method described in Section 2 is applied with two sequences of images acquired just before and after the impact in order to detect the displacements induced by the impact. The binarization threshold is fixed such that the very short delay of the measure ensures not to take into account displacements coming from the relaxation dynamics. Several realizations are performed for each pile slope and the binary images obtained for each realization are averaged in order to obtain a gray-scale picture of the local probability of displacement.

Two typical responses obtained for pile slopes respectively equal to $\theta = 13.2°$ and $\theta = 18.8°$ are shown in Figure 8a and b. The penetration depth of the impacted area is essentially constant in the order of $[10 - 20]$ beads diameters whatever the slope angle. It is the same thickness as the subsurface layer where the relaxation dynamics slows down. In contrast, the lateral extension strongly increases with θ and is larger uphill than downhill resulting in an asymmetrical response. The amplitude of the response is estimated by measuring the area of the impacted zone $A(\theta)$ as a function of the pile slope. As shown in Figure 8c the response increases strongly with θ and can be adjusted by a power-law in $(\theta_r - \theta)^{-0.5}$. Note that, given the almost constant depth of the impacted area, its lateral extension essentially follows the same law. Altogether, the response of the pile to a localized disturbance enforces the idea of collective behaviours inside the subsurface layer.

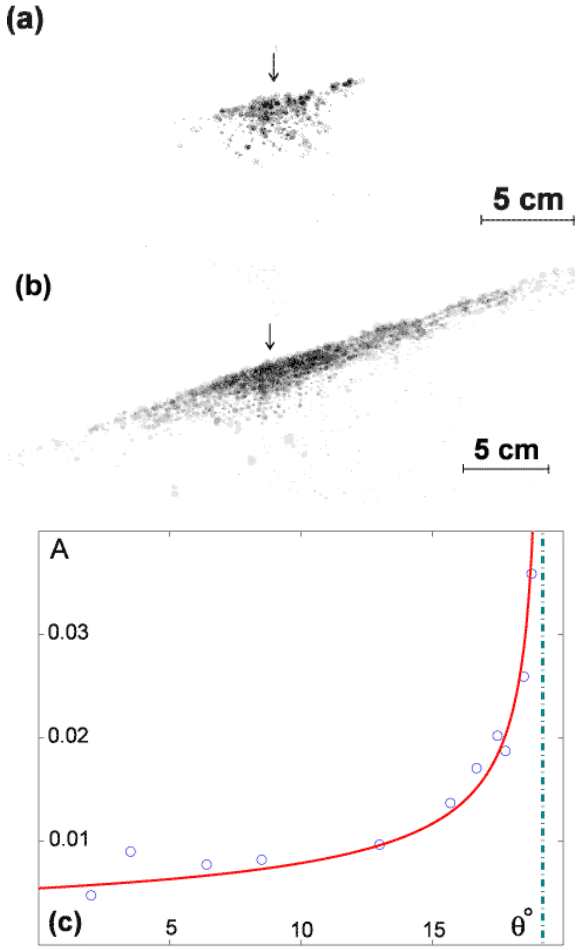

Fig. 8. Response in displacements of the pile to a bead impact. Grayscale pictures of the local probability of having a displacement for pile slopes (a) $\theta = 13.2°$ and (b) $\theta = 18.8°$; (the arrow indicates the localization of the bead impact). (c) Impacted area $A(\theta)$ as a function of the slope angle.

3.4 Summary of the experimental results

We now summarize all experimental results. Just after the occurrence of an avalanche the granular pile relaxes very rapidly – less than 15 s – in its bulk, but exhibits a much slower relaxation in a subsurface layer of thickness $[10-20]$ bead diameters. In this subsurface layer, exponential decay and reactivation bursts compete resulting in long-lived – more than 10^3 s – intermittent transients depending on the occurrence of bursts during the relaxation process. At the bead scale, the exponential decay consists in fast and small isolated displacements, whereas the reactivation bursts are related to correlated moves of beads into clusters. The exponential decay time $\tau_\downarrow$ increases from 50 s to 250 s like $(\theta_r - \theta)^{-1}$. The typical time interval separating two bursts is $\tau_b \approx 100$ s. Accordingly, the probability of having at least one burst becomes significant when $\tau_\downarrow$ becomes in the order of τ_b, that is for $\theta \approx 10°$. $N(t_w, t)$, the average number of displacements per pixel seemingly saturates exponentially on a time-scale τ increasing with the pile slope. Finally the impacted area after a perturbation

is reminiscent of the correlated domains observed during the relaxations. These results contribute to the general observation that the surface layer tends to form dynamical clusters, when driven out of mechanical equilibrium. The typical length-scale of these clusters increases with the pile slope up to several tenth of grain diameters.

4 Further analysis

4.1 Motivation and choice of description

In Section 3.3, we have assumed a scaling for $N(t_w, t)$, and used it to extract a relaxation time-scale. However this scaling is suggested by irreversible dynamics considerations, whereas direct observations clearly demonstrate the existence of reactivations. Looking for the origin of these slow dynamics has to be considered in the context of micro-mechanics, and is out of reach of the present study. In the following our less ambitious but achievable goal is first to clarify the formalism underlying the above scaling. Second, we want to investigate the possible emergence of another scaling when one includes – in the same formalism – reversible processes. We thus propose a description in which the average number of moves $N(t_w, t)$ can be computed analytically.

Assume that beads can be in two distinct kinds of states, namely a few active states labeled from 1 to n and one inactive state labeled 0. In an active state, a bead spontaneously "moves" to any other state with a total rate (probability per unit time) γ. Part of these moves occurs towards the inactive state with a rate $\alpha < \gamma$. These transitions are to be associated to physical displacements (or individual relaxations), and their average number is thus the analog of the experimentally measured quantity $N(t_w, t)$. On the contrary, beads in the inactive state cannot evolve spontaneously, and thus do not contribute to $N(t_w, t)$. Within such a description, the average number of moves is given by:

$$N(t_w, t) = \int_{t_w}^{t_w+t} \gamma P_m(t) dt, \tag{3}$$

where $P_m(t)$ is the fraction of active beads. Introducing the probability $P_i(t)$ to be in state i at time t ($i = 0 \dots n$), $P_m(t)$ is given by $P_m(t) = \sum_{i=1}^{n} P_i(t)$ and follows the simple relaxation equation:

$$\frac{d\,P_m}{d\,t} = -\alpha P_m. \tag{4}$$

Accordingly the average number of moves is:

$$N(t_w, t) = \frac{\gamma}{\alpha} P_m(0) e^{-\alpha t_w} (1 - e^{-\alpha t}), \tag{5}$$

thus recovering the scaling introduced in Section 3.4 with $\tau = 1/\alpha$.

To include the reactivation process in the description, randomly chosen beads – independently of their state – are set in an active state, with a probability ν per bead and time unit. If the chosen bead is already in an active state, this reactivation process has no effect. The reactivation mechanism itself is considered not to involve any displacement of the bead, but rather an instantaneous collective rearrangement of its environment. This ensures the validity of equation (3), for the computation of $N(t_w, t)$. Finally, thermal noise being irrelevant for granular media, it is reasonable to think that the reactivation process is driven by some mechanical noise self-generated by the relaxation of the other beads. This effect can be taken into account by imposing that the rate ν of reinjection depends, in a mean-field spirit, on the global number of active beads: $\nu = \nu(P_m)$. We consider here only the simplest functional dependence: $\nu = \mu P_m$, where μ is a constant. $P_m(t)$ then follows the evolution equation:

$$\frac{d\,P_m}{d\,t} = -\alpha P_m + \nu(P_m) P_0 = -\alpha P_m + \mu P_m\,(1 - P_m)\,, \tag{6}$$

where the second r.h.s. term accounts for the reactivations starting from the inactive state. Solving this equation leads to:

$$P_m(t) = \frac{1}{\mu} \frac{d \ln g}{d\,t}, \tag{7}$$

and

$$N(t_w, t) = \frac{\gamma}{\mu} \ln \left(\frac{g(t_w + t)}{g(t_w)} \right), \tag{8}$$

where an auxiliary function $g(t)$ has been introduced:

$$g(t) = (\alpha - \mu) + \mu P_m(0) \left[1 - e^{-(\alpha - \mu)t} \right]. \tag{9}$$

4.2 Data (re)-analysis

The scaling (8) obtained when taking into account the reactivation mechanism is functionally very different from the one obtained within the pure irreversible scenario. Does it apply to the experimentally measured $N(t_w, t)$? Whereas the above expressions depend on four parameters α, γ, μ, the transition rates and $P_m(0)$, the initial fraction of active beads, $N(t_w, t)$ actually depends on three parameters only $\gamma_P = \gamma P_m(0)$, $\delta = \alpha - \mu$ and $\mu_P = \mu P_m(0)$. Extracting these parameters from the experimental data by a unique least-square fit of the full 2-variable measurement of $N(t_w, t)$ for each type of relaxation (i.e. monotonous and intermittent) leads us to estimate the parameters written on the left side of Table 1. Figure 9 explicitly demonstrates the quality of the rescaling obtained for $N(t_w, t)$ as a function of $g(t_w + t)/g(t_w)$.

We further estimate $P_m(0)$ by imposing the ratio $\eta = \frac{\gamma}{\alpha}$ in the case of the simple exponential decay. This ratio is the averaged number of moves per bead and can reasonably be set to $\eta = 1$ by considering that the exponential decay dynamics is precisely obtained when each bead simply relaxes once from the active state to the inactive one. The obtained value $P_m(0) = 0.54$ is then imposed a priori to both dynamics. This allows to determine the elementary timescales $1/\alpha$ and $1/\delta$ for both dynamics as well as η in the intermittent dynamics (see right of Tab. 1). These

Table 1. Parameters values extracted from the experimental data for each type of relaxation: (a) the exponential decay and (b) the intermittent dynamics. Left: direct estimation of the parameters by a unique least-square fit of $N(t_w, t)$. Right: relaxation time scales $1/\alpha$ and $1/\delta$, and average number η of moves per beads (see text for details).

	(a)	(b)		(a)	(b)
γ_P	0.0096	0.0087	$1/\alpha$	56 s	294 s
δ	0.0134	0.0008	$1/\delta$	75 s	1250 s
μ_P	0.0023	0.0014	η	1	4.7

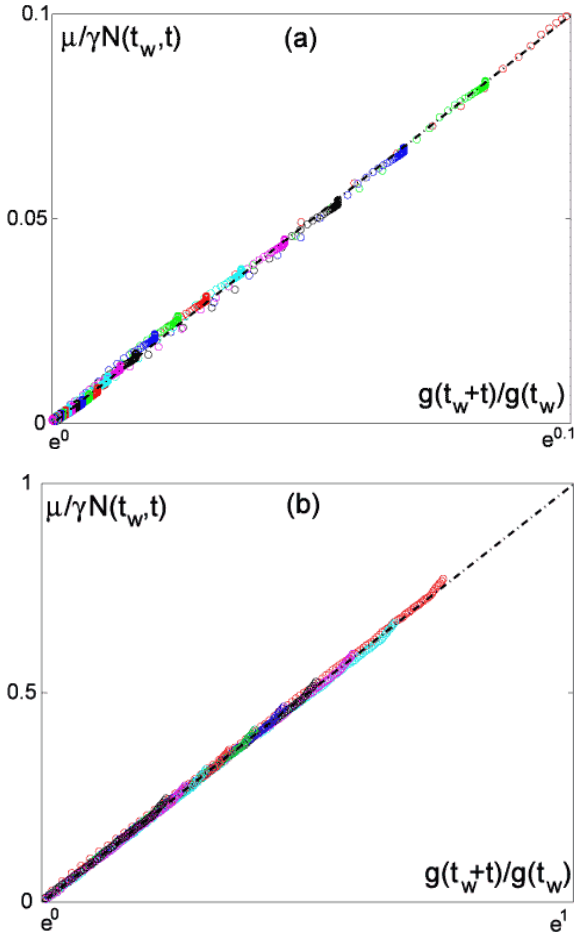

Fig. 9. $\frac{\mu}{\gamma}N(t_w, t)$ as a function of $g(t_w+t)/g(t_w)$ for each type of relaxation: (a) the exponential decay and (b) the intermittent dynamics.

values are in very good agreement with the direct observations: $1/\alpha$ varies typically between 50 s and 300 s as given by the direct measurement of the exponential decay rate displayed in Figure 6a. In the same way, $1/\delta$ is perfectly representative of the total duration of the relaxation process, namely of the order of $1/\alpha$ in the case of the exponential decay and larger than 10^3 s when intermittent bursts occur. Finally, $\eta = 4.7$ is a reasonable value for the average number of moves per bead in the sense that it agrees well with the average number of bursts during an intermittent relaxation. Altogether, despite its simplicity, our model based on elementary dynamical processes provides a good description of the relaxation dynamics.

5 Discussion

We now plan to discuss the above observations and the analysis conducted on the experimental data, before suggesting some parallel with aging behaviours in the general context of glassy materials.

The strongest experimental result is obviously the observation of unexpected non trivial relaxations, during which reactivations occur in the form of correlated beads clusters involving rather long relaxation times ($\tau_\downarrow \in [50\text{ s}, 300\text{ s}]$ and $\tau_b \simeq 100$ s) compared to the only characteristic time defined at the bead scale, $\sqrt{d/g} \approx 10^{-2}$ s. Looking for the origin of these slow dynamics has to be considered in the context of micro-mechanics, and is out of reach of the present study. Still, recent numerical studies [10,11] reveal the existence of two types of constitutive structures, namely the strong forces chains network and the critical contacts clusters. Whereas the characteristic size of the former remains constant, the size of the latter increases with θ. These results suggest an intuitively appealing, although rather speculative parallel. The fact that τ_b is constant could be a fingerprint of the underlying role played by the strong force network. Conversely, the increase with θ of the monotonous relaxation time $\tau_\downarrow$ might be associated with the growth of the critical clusters. In this perspective, the length-scale characterizing the spatial response to a localized disturbance may be identified with the characteristic size of the critical clusters observed numerically. However, at the present stage, the precise connection between the existence of spatially correlated clusters and the observed timescales remains unclear. Further numerical studies of these collective mechanisms are under progress. Also, one must envision the possible role played by alternative mechanisms such as creeping, ruled by microscopic properties of the beads such as their surface state.

Having measured the two-time relaxation function, we have introduced a simple description, which allows to clarify the necessary hypothesis underlying the calculation of $N(t_w, t)$. In this context, we recover two interesting scalings. In the first case, neglecting the description of the reactivation processes, one obtains the expected exponential saturation, with a unique characteristic time-scale τ. This simple scaling correctly describes the experimental data for $N(t_w, t)$ but suffers some important weaknesses. The most obvious one is that it neglects by construction the reactivation processes, which are clearly evidenced by direct observations. Second, it leads to a time-scale τ which varies from 73 s to 725 s. Whereas the shortest one is indeed in the order of the exponential decay rate observed at small angle $\tau_\downarrow \simeq 50$ s, the largest one is twice larger than the exponential decay rate measured between the reactivations at large angle $\tau_\downarrow \simeq 300$ s. Of course, τ could be some effective time, taking implicitly into account the slowing

down of the dynamics induced by the reactivations. But, in this interpretation, the scaling is not "trivial" anymore and escapes the present framework of description. Alternatively, we have proposed to add a description of the reactivations in the same formalism, with minimal hypothesis. It leads to a scaling, which compares as well with the experimental data. It looks a bit complicated, but offers significant benefits. Apart from the fact that it includes the reactivation processes, it provides two time-scales: $1/\alpha$ associated to the exponential decay and $1/\delta$ corresponding to the total duration of the relaxation. Moreover these estimates are in very good agreement with the measured equivalent quantities. Finally, as we discuss below, it significantly enlarges the perspective of the present study. It relates our observations to some aging behaviour in granular media, calling for further connections with other glassy systems.

It is worth noticing that at the qualitative level the observed dynamics, with a competition between irreversible relaxation and reactivation events, has in fact a much wider validity than the present experimental system. Such a scenario can be also invoked generically in the case of soft glassy materials (foams, pastes, slurries), in which local relaxation of stress competes with a mechanical noise generated by the relaxation of the surrounding structures [12,13]. Experimental evidence for intermittent events in the relaxation of polymers has also been found recently [14]. Thus the following question arises: given the above two processes as basic ingredients, could one expect a somewhat generic behaviour for these athermal dissipative systems, as it is the case for thermal glassy materials which often exhibit an aging scaling in $(t_w + t)/t_w$ of their correlation function $C(t_w, t)$? It is thus of interest to calculate in the above formalism the correlation function $C(t_w, t)$ defined as the probability not to have changed state between t_w and $t_w + t$. This correlation decomposes into the sum of the probability not to move starting from an active state at t_w and the probability not to be reactivated given that the bead was inactive at t_w:

$$C(t_w, t) = P_m(t_w)e^{-\gamma t} + [1 - P_m(t_w)]\frac{g(t_w)}{g(t_w + t)}. \quad (10)$$

One could expect $C(t_w, t)$ to exhibit the typical two-step relaxation form, familiar to the glass community. However, the first step of the relaxation is hard to evidence since its relative contribution is given by $P_m(t_w)$, which vanishes as t_w increases, so that we mainly focus on the second step of the relaxation. Interestingly, the corresponding term presents a scaling form, which depends only on the rescaled function $g(t_w + t)/g(t_w)$. This scaling form is precisely the generic aging form proposed by Cugliandolo and Kurchan [15], to generalize the simple aging scaling in $(t_w+t)/t_w$ by introducing a reparametrization of time $g(t)$.

Figure 10 displays the relaxation of the aging-like term $h(t_w, t) = [g(t_w + t)/g(t_w)]^{-1}$, for several t_w and for two different sets of parameters. The characteristic time t_0 associated to the decay of $h(t_w, t)$, for a given t_w can be identified with the inflexion point of $h(t_w, t)$ when plotted as a function of $\ln t$. Several regimes have to be distinguished according to the value of t_w. For $t_w \ll 1/\delta$, one finds $t_0 = 1/\mu P_0 + t_w$ (which can be approximated by $1/\alpha + t_w$), whereas for $t_w \gg 1/\delta$, t_0 saturates to the value $1/\delta$. In Figure 10a, the parameters are set to arbitrary values such that time scales are widely separated, so as to evidence the three regimes described above. One clearly observes the simple aging behaviour (i.e. $t_0 \approx t_w$) in the time window $1/\alpha \ll t_w \ll 1/\delta$. One may also notice the strong increase of the plateau value when t_w reaches $1/\delta$ due to the fact that $g(t)$ *saturates* for large t instead of diverging. Figure 10b displays the same function using the parameters values given in Table 1, in order to extrapolate to large times the experimental data. The results are similar, in particular concerning the behaviour of the plateau, but the intermediate aging regime is much less obvious, because of the weaker time-scale separation between $1/\alpha$ and $1/\delta$. The saturation of $g(t)$ makes the scenario in the present model appear a bit different from the full aging case: aging is interrupted beyond a certain time scale, and the correlation function does not decay to zero, but rather to a plateau value depending on t_w, which goes to 1 when $t_w \to \infty$. Although this behaviour might seem surprising

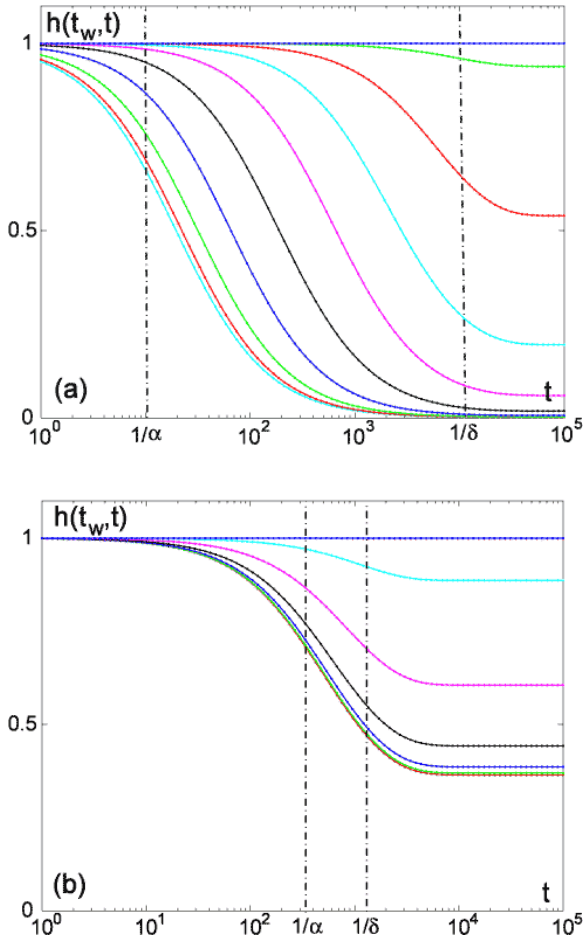

Fig. 10. $h(t_w, t)$ as a function of $\ln t$, for different t_w and for two sets of parameter values: (a) arbitrary values $1/\alpha = 10$ s, $1/\delta = 10^4$ s and (b) experimentally obtained values $1/\alpha = 294$ s, $1/\delta = 1250$ s.

at first sight, its interpretation is clear: the global activity of the system vanishes at long times, so that decorrelation is harder and harder to achieve.

6 Conclusion

In this paper, we have studied the relaxation of a granular pile following an avalanche. We briefly consider the statistics of the angle of the pile $\theta(t)$ in the avalanching regime, measuring in particular the histograms of the starting angle θ_{start} and of the stopping angle θ_{stop}, from which we evaluate the angle of repose of the pile.

The major experimental result is the observation and the quantitative characterization of unexpected long-lived transients. Quantifying the 'activity' in the pile with $\delta A(t)$ by comparing subsequent images, we find two different kinds of dynamics, namely monotonous exponential decays and intermittent reactivations related to spontaneous correlated displacements of beads, with both a characteristic time in the order of 10^2 s. The competition between these two dynamics generates long transients lasting for more than 10^3 s. The correlated bursting events are localized in a subsurface layer of 10 to 20 beads diameters thickness. Interestingly, whereas the typical time τ_b elapsed between two bursts remains constant when varying the slope θ of the pile, the exponential relaxation time $\tau_\downarrow$ increases sharply when θ approaches the angle of repose θ_r. As a result of this slower exponential decay, the probability to observe intermittent bursts during the relaxation also increases with θ. Finally, measuring the instantaneous response of the pile to a localized perturbation has contributed to the identification of the typical length-scales involved in the observed spatial correlations.

In order to investigate such a non-stationary process, we have measured the two-time relaxation function $N(t_w, t)$, the average number of detected moves between times t_w and $t_w + t$. This function has been analysed within a well defined description. We could show that the experimentally measured $N(t_w, t)$ may well be fitted by two different scalings. However, given the direct observations of the reactivation bursts and the quantitative measurements performed on the relevant time-scales, we believe that the scaling obtained when including the reactivations provides the best overall consistency.

Finally, computing in this context a natural correlation function, we show that it behaves essentially in an aging-like manner, as a function of $g(t_w + t)/g(t_w)$, where $g(t)$ can be interpreted as a reparametrization of time which saturates for large times so as to account for the full dynamical arrest. This may be considered as a general scenario for the long time dynamics of (non driven) athermal jamming systems, in which local relaxation competes with a mechanical noise generated by the relaxation of the surrounding structures.

The authors gratefully acknowledge J.P. Bouchaud for fruitfull discussions and F. Daviaud and D. Bonamy for valuable advices on the use of the experimental set up.

References

1. P. Bak, C. Tang, K. Wiesenfeld, Phys. Rev. Lett. **59**, 381 (1987)
2. P. Evesque, J. Rajchenbach, C. R. Acad. Sci. Paris **307**, 223 (1988)
3. H.M. Jaeger, C.H. Liu, S.R. Nagel, Phys. Rev. Lett. **62**, 40 (1989)
4. C.H. Liu, H.M. Jaeger, S.R. Nagel, Phys. Rev. A **43**, 7091 (1991)
5. Y. Grasselli, H.J. Herrmann, Physica A **246**, 301 (1997)
6. S. Courrech du Pont, P. Gondret, B. Perrin, M. Rabaud, Phys. Rev. Lett. **90**, 044301 (2003)
7. D. Bonamy, S. Bernard-Bernardet, F. Daviaud, L. Laurent, Phys. Rev. E **68**, 042301 (2003)
8. J. Rajchenbach, Phys. Rev. Lett. **65**, 2221 (1990)
9. M. Caponeri, S. Douady, S. Fauve, C. Laroche, *Dynamics of avalanches in a rotating cylinder*, in *Mobile particulate systems,* edited by E. Guazzelli, L. Oger (Dordrecht, Kluwer Academic Publisher, 1995), pp. 331–366
10. L. Staron, J.P. Vilotte, F. Radjai, Phys. Rev. Lett. **89**, 204302 (2002)
11. F. Radjai, D.E. Wolf, M. Jean, J.J. Moreau, Phys. Rev. Lett. **80**, 61 (1998)
12. P. Hebraud, F. Lequeux, Phys. Rev. Lett. **81**, 2934 (1998)
13. P. Sollich, F. Lequeux, P. Hebraud, M.E. Cates, Phys. Rev. Lett. **78**, 2020 (1997)
14. L. Buisson, S. Ciliberto, A. Garcimartin, Europhys. Lett. **63**, 603 (2003)
15. L.F. Cugliandolo, J. Kurchan, J. Phys. A **27**, 5749 (1994)